Response Surface Modeling for Networked Radar Resource Allocation

Allan De Freitas*, Richard W. Focke§, Pieter de Villiers*
*University of Pretoria, South Africa
§ Council for Scientific and Industrial Research, South Africa
Emails: *a.defreitas@tuks.co.za, rfocke@csir.co.za, pieter.devilliers@up.ac.za*

***Abstract*—Sensor management is an important function of any data fusion center as the output of a fusion system is dependent on the quality of the information collected. In this paper, the scheduling aspect of sensor management function is implemented using Response Surface Modeling (RSM). Applying RSM requires formulating the sensor management function as an objective function. The benefit of RSM over prior global optimization approaches is the simplification of the evaluation of this objective function to find global optima. This leads to either reduced computational requirements and/ or shorter due times for creating sensor schedules.**

This work shows the utility of RSM towards scheduling multiple sensors, and seeks to introduce RSM to the sensor management community. It is shown that the RSM scheduler provides a significant improvement towards reducing the number of missed targets in a surveillance radar network. This is compared to performing a uniform scanning regime (or sequential stepped scan) often employed. Very few iterations are required to provide this gain. The RSM technique also quickly determines where the most effective use of sensor resources needs to be applied. Consequently, it spends more radar dwell time on these beam locations.

***Index Terms*—Process Refinement, Sensor management, Scheduling, Radar Networks, Surveillance, Response Surface Modeling**

I. Introduction

Sensor management is part of the Data Fusion Model proposed by the Data Fusion Information Group (DFIG) [1]. A sensor management algorithm must perform three important tasks: creation of suitable sensor tasks, prioritization of these tasks and, finally, scheduling of tasks on the sensors. Prior to formulating a sensor management solution it is important to model the sensors and their role in the fusion system. The approach followed in this paper is detailed in Section II. Thereafter, a solution should be implemented, and it is important to consider the architecture, which is the focus of much recent work [2], [3], [4], [5] but not addressed as part of this work. Task creation and prioritizing tasks, while important, for this work are achieved by using simple heuristics derived from sensor operator intuition. The focus in this work is on presenting response surface modeling (RSM) as a suitable multisensor scheduling algorithm.

RSM has long been used to solve challenging optimization problems where objective functions are expensive to evaluate [6], [7]. The taxonomy presented in [7] has recently been popularized in the artificial intelligence community from a Bayesian perspective by [8]. The principal premise of RSM is to create a surrogate model of the objective function by using as few as possible objective function evaluations. An additional advantage of response surface methods, is that when using Gaussian process (kriging) interpolation [9] and a suitable acquisition function [8], the optimization algorithm balances the optimization task (minimizing the surrogate objective function), with the objective function sampling task (choosing where to sample the objective function to reduce uncertainty in the surrogate model). This allows the optimizer to balance the task of "exploring" with "exploiting" the objective function, while at the same time utilizing the statistical uncertainties in the surrogate model to improve joint optimization and sampling.

The application of RSMs to resource optimization in the literature is scarce. The authors of [10] consider the use of an RSM applied to resource optimization advanced manufacturing application. A RSM is used to optimally allocate resources for the improved food production in [11]. In [12], a RSM is used for selecting an optimal set of sensors, as determined by predictive accuracy and other sensor performance parameters. This is in contrast with this paper, which uses dwell time to minimize the probability of a missed detection of multiple sensors. The efficient use of resources for robot path planning and sensing is achieved using a RSM in [13].

Sensor scheduling approaches must treat the sensor resources against a timeline of suitable slots, where only a single task using a specific sensor or sensor resource may occupy a slot on the utilization timeline. Sensor scheduling approaches are summarized in [14], [15], [16]. Heuristic schedulers have dominated the approaches from early work such as [17] to more recent approaches such as [18], [19], [20], [21]. Sometimes the scheduling is handled intrinsically by the task prioritization algorithm [22], [23] including Bayesian approaches [24], or as outputs of the other sensor functions [25], [26]. These approaches are good at solving a single problem formulation, but are not easily extensible to different scenarios and often required much analysis to rework.

The scheduling problem can also be formulated as an optimization problem as is done in Section III. Then the use of various optimization algorithms as the scheduler becomes possible. Mathematical programming approaches to solving information-theoretic approaches are one option [27], [28]. Alternatively, artificial intelligence approaches such as genetic algorithms and particle swarm optimization have also been proposed [29], [30], [31], [32] as well as using both in a hybrid algorithm [33]. Another option is techniques such as online Monte Carlo simulations [34]. These approaches suffer from heavy computational burden and long times to reach a globally optimal solution. RSM allows the computational load to be managed through model simplification and does not require long runs to reach a global optima in the solution space as shown in Section IV. Furthermore, RSM schedulers that employs a good architecture merely requires the formulation of the sensor management problem as an optimization problem to apply to new sensor suites.

II. Target Surveillance Model

Consider a networked radar system with the primary function of detecting targets. Search radar systems are designed with the aim of detecting targets in their surveillance space. However, radar systems operate with limited resources, which inherently restricts the system from continuously observing the entire search space. Typically a set amount of time is allocated to scanning the entire region, referred to as the scan time. The mechanism of scanning is dependent on the sensor, i.e. mechanically steered, or electronically steered. In this paper, the case where the search space of a radar is subdivided into a set of non-overlapping regions is considered.

A. Poisson Point Processes Formulation

A Poisson point process (PPP) is a useful mathematical tool which has been applied in a wide variety of applications. An inhomogeneous PPP with intensity function $\lambda(\cdot)$ is a point process in $\mathbb{R}^n$ such that: for every subset of the space, $A \subseteq \mathbb{R}^n$, the number of counts, $N(A)$ has a Poisson distribution with parameter $\lambda(A) = \int_A \lambda(x)dx < \infty$; and for any collection of disjoint bounded Borel measurable sets $A_1, \ldots, A_n \subseteq A$, $N(A_1), \ldots, N(A_n)$ are independent [35].

In this paper, a PPP is used to represent the number of undetected targets. Thus, if the search space is denoted by the region A, then $N(A)$ is the number of undetected targets. The search space is represented by a discrete set of non-overlapping cells, $\mathcal{S} = \{\mathcal{S}_1, \cdots, \mathcal{S}_N\}$. This results in a PPP with a discrete intensity function. It is also noted that the number of undetected targets varies with time. The time dependence is reflected by the discrete intensity function, which is represented mathematically by $\lambda_{k|k}(\mathcal{S}_i; \boldsymbol{\alpha}_k)$, where $k \in \{1, 2 \ldots T\}$ the discrete time steps, with T representing the final time step. The intensity is also dependent on the system parameters, which are represented by $\boldsymbol{\alpha}_k$. It has been shown in [36] that the intensity function of each cell can be iteratively updated to maintain an estimate of the number of undetected targets as time progresses. This is achieved through a two step procedure. The first step is given by

$$\lambda_{k|k-1}(\mathcal{S}_j; \boldsymbol{\alpha}_{k-1}) = \lambda_b(\mathcal{S}_j) + \sum_{i|\mathcal{S}_j \in \mathcal{T}(\mathcal{S}_i)} P(\mathcal{S}_j|\mathcal{S}_i) P_s(\mathcal{S}_i) \lambda_{k-1|k-1}(\mathcal{S}_i; \boldsymbol{\alpha}_{k-1}), \tag{1}$$

where $\lambda_{k-1|k-1}(\mathcal{S}_j; \boldsymbol{\alpha}_{k-1})$ is the intensity function of cell $\mathcal{S}_j$ at time step $k-1$ based only on information from time step $k-1$; $\lambda_b(\mathcal{S}_j)$ is the intensity function of a PPP, which models the number of undetected targets entering the region at time k, referred to as births; $P(\mathcal{S}_j|\mathcal{S}_i)$ represents a transition distribution induced by the Markov kernel $p(\boldsymbol{x}_k|\boldsymbol{x}_{k-1})$ on $\boldsymbol{x} \in A$; $\mathcal{T}(\mathcal{S}_i)$ is the subset of cells to which a target can transition from cell $\mathcal{S}_i$ (so that $P(\mathcal{S}_j|\mathcal{S}_i) = 0 \forall \mathcal{S}_j \notin \mathcal{T}(\mathcal{S}_i)$); $P_s(\mathcal{S}_i)$ represents the survival probability of undetected targets at $k-1$ in cell $\mathcal{S}_i$ to time k; and $\lambda_{k|k-1}(\mathcal{S}_j; \boldsymbol{\alpha}_{k-1})$ is the intensity function of cell $\mathcal{S}_j$ at time step $k-1$ updated by the aforementioned terms. The second step is given by

$$\lambda_{k|k}(\mathcal{S}_j; \boldsymbol{\alpha}_k) = (1 - P_D(\mathcal{S}_j; \boldsymbol{\alpha}_k))\, \lambda_{k|k-1}(\mathcal{S}_j; \boldsymbol{\alpha}_{k-1}), \tag{2}$$

where $P_D(\mathcal{S}_j; \boldsymbol{\alpha}_k)$ represents the probability of detecting a target in cell $\mathcal{S}_j$.

In this paper, the search system is assumed to consist of multiple radars which may include areas of overlap. The probability of detection is based on the inclusion-exclusion principle applied to the probability of detection of each radar. This is illustrated for the two radar scenario, but can be adapted to any number of radars:

$$P_D(\mathcal{S}_j; \boldsymbol{\alpha}_k) = P_{D,1}(\mathcal{S}_j; \boldsymbol{\alpha}_k) + P_{D,2}(\mathcal{S}_j; \boldsymbol{\alpha}_k) - P_{D,1}(\mathcal{S}_j; \boldsymbol{\alpha}_k) P_{D,2}(\mathcal{S}_j; \boldsymbol{\alpha}_k) \tag{3}$$

where $P_{D,x}(\mathcal{S}_j; \boldsymbol{\alpha}_k)$ represents the probability of detection for radar x, and the probability of detection of the individual radars is assumed independent.

III. Global Optimization

In general, optimization is the process of determining the parameters which result in a minimum of a function, referred to as the objective function. In this paper, the objective function is the expected number of undetected targets for the search space given by

$$f(\boldsymbol{\alpha}_k) = \sum_{i=1}^{N} \lambda_{k|k}(\mathcal{S}_i; \boldsymbol{\alpha}_k). \tag{4}$$

The corresponding optimization problem is given by

$$\boldsymbol{\alpha}_k^* = \arg \min_{\boldsymbol{\alpha}_k \in \mathcal{X}} f(\boldsymbol{\alpha}_k) \quad \text{s.t.} \quad c(\boldsymbol{\alpha}_k) \leq 0 \tag{5}$$

where $\mathcal{X}$ is a subset of $\mathbb{R}^D$, and $c(\boldsymbol{\alpha}_k)$ is a known constraints function.

Optimization is a challenging task as the objective function may consist of many local minima within the search space. In addition, objective functions in complex systems can be computationally expensive to evaluate, without closed form expressions of gradients. For example, in the case of a search radar system with a model for probability of detection which considers complex targets, spatial diversity, and clutter. The aim of a global optimization algorithm is to search for the global minima. The approach proposed for global optimization in this context is based on the concept of RSM [7]. A response surface represents a computationally cheap surrogate of the objective function which can be used for global optimization. In this paper, the response surface is approximated with a Gaussian Process (GP) regression model.

A. Gaussian Process Regression

A GP is a stochastic process that is suitable for modeling non-linear functions. GPs can be described as a distribution over functions [37]. This distribution is characterized by a mean function, $m(\boldsymbol{x})$, and covariance function, $k(\boldsymbol{x}, \boldsymbol{x'})$,

$$\begin{aligned} m(\boldsymbol{x}) &= \mathbb{E}[f(\boldsymbol{x})] \\ k(\boldsymbol{x}, \boldsymbol{x'}) &= \mathbb{E}[(f(\boldsymbol{x}) - m(\boldsymbol{x}))(f(\boldsymbol{x'}) - m(\boldsymbol{x'}))], \end{aligned} \tag{6}$$

resulting in the following expression for a GP

$$g(\boldsymbol{x}) \sim \mathcal{GP}(m(\boldsymbol{x}), k(\boldsymbol{x}, \boldsymbol{x'})). \tag{7}$$

A GP is a collection of random variables, any finite set of points, i.e. $\{\boldsymbol{x}_i \in \mathcal{X}\}_{i=1}^M$, induces a consistent joint Gaussian distribution on $\mathbb{R}^M$. This property of the GP is used to obtain closed form expressions for marginals and conditionals, such as the posterior.

The mean function prior is typically assumed equal to zero or constant. This places a large importance on the model selected for the covariance kernel, as well as on the hyperparameters of the model. They are commonly learned by maximizing the conditional likelihood [37].

B. Global Optimization with Response Surface Modeling

RSM is a global optimization method based on a statistical approach[1]. A probabilistic model is used to represent the objective function. In this paper, it is modeled with a GP[2]. Using a GP based model has the advantage of a closed form expression to quantify uncertainty.

Initially, there are no observations from the objective function. Each time the objective function is evaluated, also referred to as an optimizer iteration, the observation is stored, i.e. $\{\boldsymbol{\alpha}_k^{(v)}, y(\boldsymbol{\alpha}_k)^{(v)}\}_{v=1}^V$, where $y(\boldsymbol{\alpha}_k) \sim \mathcal{N}(f(\boldsymbol{\alpha}_k), \nu)$,and V is the number of stored observations. The observations are used to obtain a model posterior. Computing the model posterior based on all the observations results in an increased computational expense in comparison to optimization techniques that only consider local gradient information. However, this allows the model to converge to a global solution with a small number of objective function evaluations even for challenging non-convex objective functions [7].

After computing the posterior model, the next point in the search space for objective function evaluation is selected as the point which maximizes an acquisition function. Several acquisition functions have been described, one such function evaluates the expected amount of improvement of the objective function in the search space, represented mathematically as [7]

$$EI(\boldsymbol{\alpha}_k) = \sigma(\boldsymbol{\alpha}_k)[u\Phi(u) + \phi(u)], \tag{8}$$

[1]In the context of utilizing GP prior functions, this method has also been referred to as Bayesian optimization (e.g. [8])

[2]A summary of the algorithm for a single radar scan is illustrated in the Appendix.

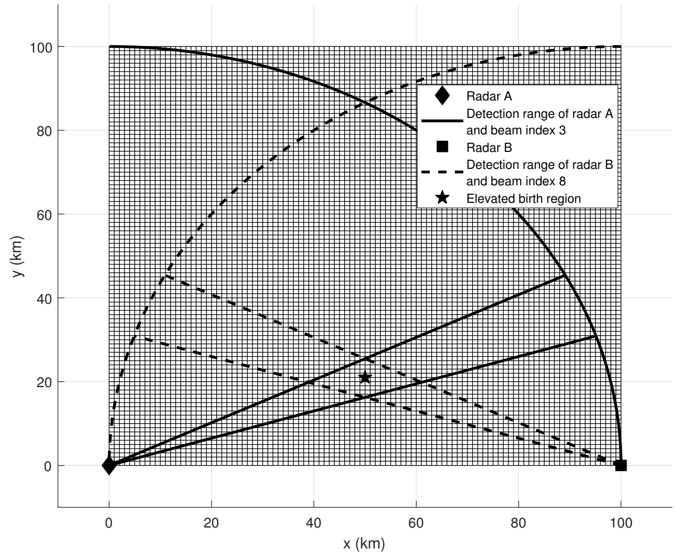

Fig. 1: Geometry of the simulation scenario.

where $u = \frac{f_{\min} - \mu(\boldsymbol{\alpha}_k)}{\sigma(\boldsymbol{\alpha}_k)}$, Φ and ϕ represent the normal cumulative distribution function and density function, respectively, $\sigma(\boldsymbol{\alpha}_k)$ and $\mu(\boldsymbol{\alpha}_k)$ represent the predictive mean function and standard deviation function, respectively, and $f_{\min}$ is the current best objective function observation.

IV. EXAMPLES & RESULTS

A. Example Scenario

Consider the scenario with two stationary radars[3] observing a 2-D surveillance region. The region is divided into a 100×100 Cartesian grid, with each cell in the grid has a surface area of one square kilometer. The position of each radar is $\text{P}_A(x, y) = (0, 0)$ km and $\text{P}_B(x, y) = (100, 0)$ km. The angular extent covered by each radar is $\Theta_{tot,A} = [0, \frac{\pi}{2}]$ rad and $\Theta_{tot,B} = [\frac{\pi}{2}, \pi]$ rad. The maximum range of both radars is 100 km. The angular extent of each radar is divided into 10 equally sized non-overlapping pie-slice shaped regions, each with an angular extent equal to that of the radar beam. The radar resource for optimization is the dwell time for each beam, $\boldsymbol{\alpha}_k = \{\tau_{i,j}\}_{i \in \mathcal{B}, j \in \mathcal{R}}$, where $\mathcal{B}$ and $\mathcal{R}$ represent the indexes for the beams in a radar and individual radars, respectively. The total scan time, T_{scan}, available to visit all the beams is 1 s for each radar, which leads to the constraints $\sum_{i \in \mathcal{B}} \tau_{i,j} \leq T_{\text{scan}}$ for each radar. The geometry of the scenario is illustrated in Figure 1. The birth intensity is a step-wise function

$$\lambda_b(\mathcal{S}_j) = \begin{cases} 2 & j \in \mathcal{C} \\ 10^{-3} & \text{otherwise} \end{cases} \tag{9}$$

where $\mathcal{C}$ represents the indexes for 4 cells in the region indicated in Figure 1. The initial intensity, $\lambda_0(\mathcal{S}_j)$, is equal to the birth intensity in (9).

[3]Differentiated with indexes A and B

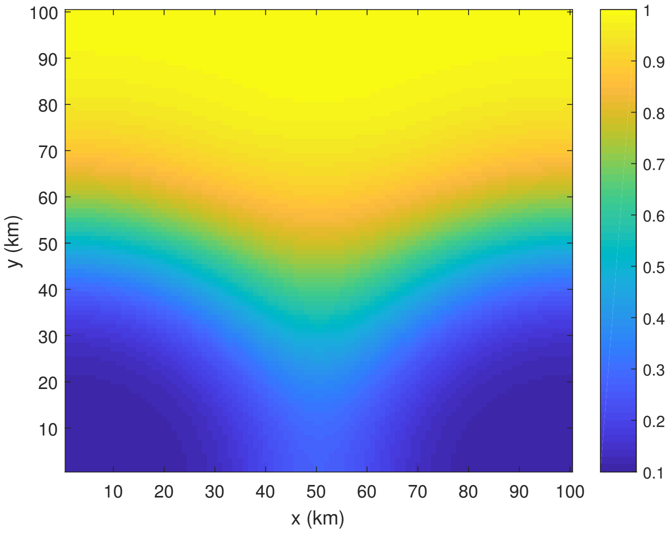

Fig. 2: Illustration of the probability of miss, $1 - P_D(\mathcal{S}_j; \boldsymbol{\alpha}_k)$, with a uniform scan time of 0.1 s for a constant radar cross-section (RCS).

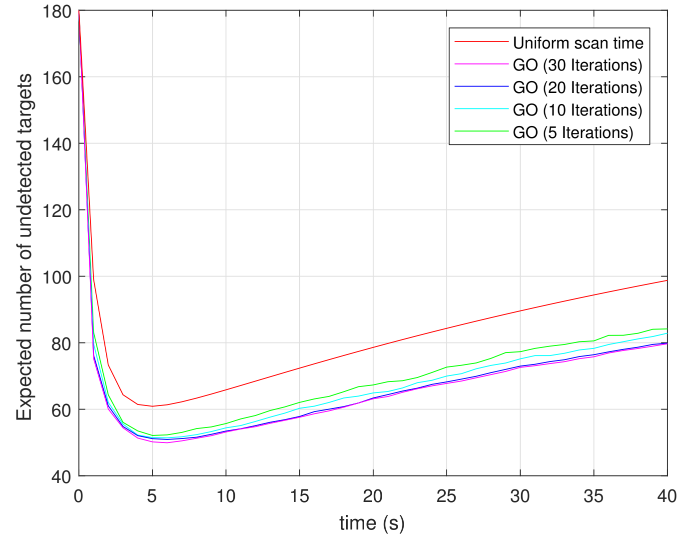

Fig. 3: Comparison of the output of the objective function for a uniform scan time and scan time optimized globally, for varying numbers of optimizer iterations.

B. Gaussian Process Model

The covariance function can significantly affect the quality of GP regression. Based on the recommendation of [8], a Matérn 5/2 covariance function is utilized.

C. Probability of Detection

A key advantage of the method presented in this paper is the ability to deal with challenging non-convex objective functions. In a search radar system, this may be caused by complex probability of detection models. In this paper, the modified Albersheim model [38] presented in [36] is used for the experiments. The probability of detection for each radar is given by

$$P_{D,x}(\mathcal{S}_j; \boldsymbol{\alpha}_k) = \frac{(1-d) + (1-\gamma)e^{b_{\mathcal{S}_j}(\boldsymbol{\alpha}_k)}}{1 + e^{b_{\mathcal{S}_j}(\boldsymbol{\alpha}_k)}}, \quad (10)$$

where $b_{\mathcal{S}_j}(\boldsymbol{\alpha}_k) = \frac{\sigma_R \tau_{i,x} - c}{0.12c + 1.7}$, $c = \log(0.62/P_{\text{fa}})$, and the probability of false alarm, $P_{\text{fa}} = 10^{-6}$, $\gamma = 0.1$ is the probability of eclipsing. The constant $d = 1 + (1-\gamma)e^{-c/(0.12c+1.7)}$ is added to fix the probability of detection to zero with zero resources. The radar cross-section of the target, σ_R parameter, decreases as the third power of the range, and is scaled so that the probability of detection for each radar is 50% with a dwell time of 0.1 s at a range of 50km. The joint radar system probability of miss for the aforementioned scenario is illustrated in Figure 2 for a dwell time of 0.1 s assigned to each beam.

D. Results

The aforementioned scenario was simulated for a total period of 40 s. The results presented are averaged over 10 independent Monte Carlo runs. The presented method is compared with a search radar system with the same geometry, but using a raster search pattern, where the total scan time is divided uniformly between the beams.

Figure 3 illustrates the objective function value for varying numbers of optimizer iterations. Regardless of the selected number of optimizer iterations, the presented method outperforms the uniform scan time approach. The reason for this is clearly demonstrated in Figure 4. The dwell time assigned to the beams for all the simulated scans are illustrated in Figures 4a and 4c for radar A and B, respectively. The dwell time for the beams observing the region of the search space with the high intensity birth cells generally have increased dwell times throughout the simulation. This is confirmed in Figures 4b and 4d, which illustrate the corresponding dwell times averaged over all simulation times. An increased dwell time in this region results in a reduction of the expected number of undetected targets. The algorithm is able to exploit the overlap of radar detection ranges by reducing the dwell time the greater the overlap, as illustrated for beam index 2 and 9 in Figures 4b and 4d, respectively.

By comparing Figures 4 and 5, the effect of varying the number of optimizer iterations is illustrated. Even with a limited number of optimizer iterations, the method is still able to allocate the majority of resources to the beams observing the cells with high birth intensity. The increased performance observed for an increasing number of optimizer iterations is offset by an increase in computational expense. The number of iterations will typically be determined by the available computational time.

Performance of the method for the case where high clutter regions exist is also considered. This is achieved by modifying the scenario depicted in Section IV-A by including 18 cells, which have a probability of detection of 0, independent of the dwell time. These cells are located in the vicinity of $(40, 5)$

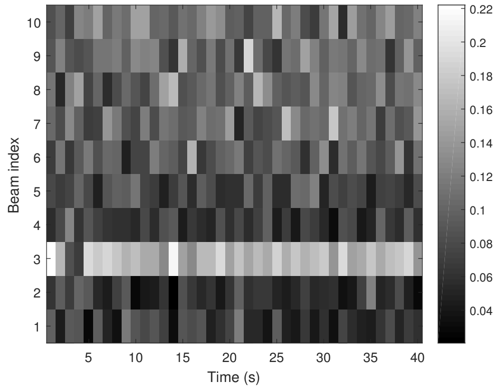

(a) Dwell time assigned to each beam represented by the intensity of the image for radar A.

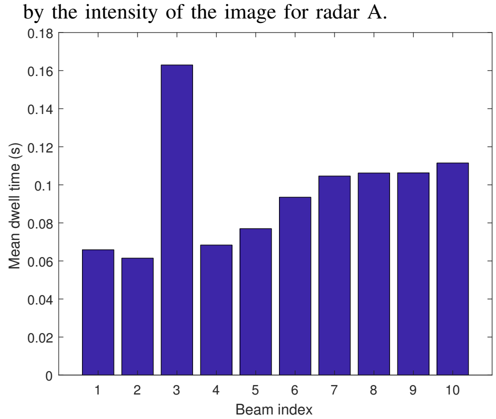

(b) Average dwell time per beam for radar A.

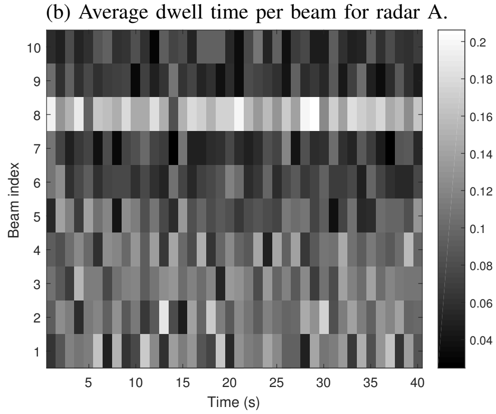

(c) Dwell time assigned to each beam represented by the intensity of the image for radar B.

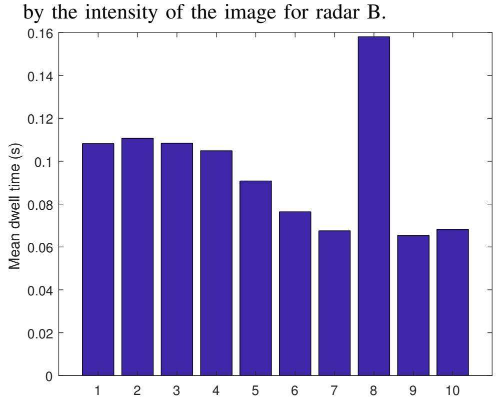

(d) Average dwell time per beam for radar B.

Fig. 4: Illustration of the optimized dwell times over a 40 s period with 30 optimizer iterations.

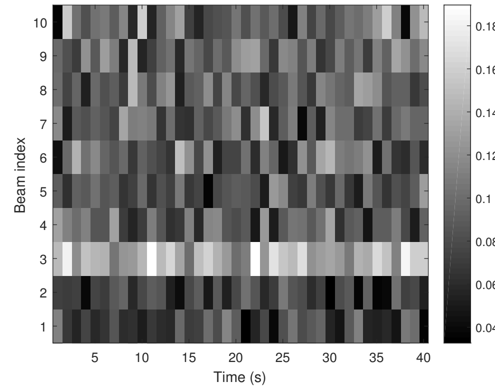

(a) Dwell time assigned to each beam represented by the intensity of the image for radar A.

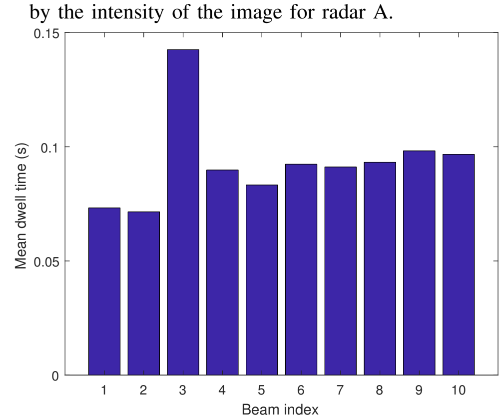

(b) Average dwell time per beam for radar A.

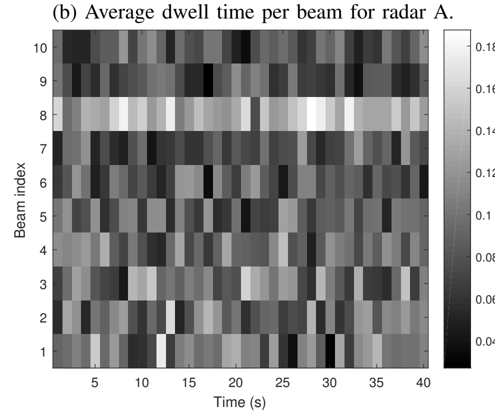

(c) Dwell time assigned to each beam represented by the intensity of the image for radar B.

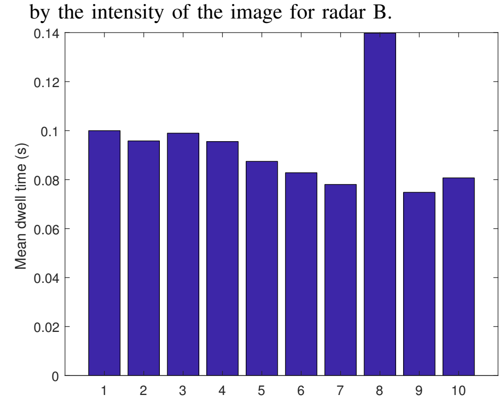

(d) Average dwell time per beam for radar B.

Fig. 5: Illustration of the optimized dwell times over a 40 s period with 5 optimizer iterations.

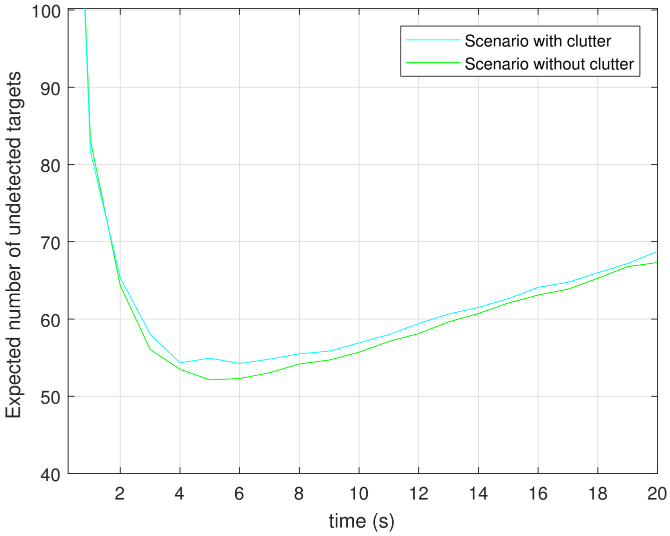

Fig. 6: Performance comparison of the presented method with 5 optimizer iterations when considering the scenario with and without the addition of clutter cells.

km on the grid presented in Figure 1. Including the clutter cells has no influence on the distribution of dwell times. This is expected as increasing the dwell time for the beams, which observe the region that includes the clutter cells, has no impact on the probability of detection. The impact of the clutter cells is noted with an increase in the number of expected undetected targets as illustrated in Figure 6.

V. Conclusions & Future Work

This work shows the utility of RSM towards scheduling multiple sensors, and introduced RSM to the sensor management community. It shows that the RSM scheduler provides a significant improvement towards reducing the number of missed targets in a surveillance radar network. This is compared to performing a uniform scanning regime (or sequential stepped scan) often employed by surveillance radars. The RSM scheduler requires very few iterations to provide a significant reduction in the number of missed targets. The RSM technique also quickly determines where the most effective use of sensor resources needs to be applied. Consequently, it spends more radar dwell time on these beam locations. The scheduler is not impacted when considering clutter regions that reduce the ability of the radar to detect targets. Future work will compare our RSM scheduler to other global optimization techniques to further demonstrate the benefit of this algorithm. Finally, mapping the RSM scheduler to a sensor management architecture is also left as future work.

Acknowledgment

The financial assistance of the ABSA Chair in Actuarial Science towards this research is hereby acknowledged. Opinions expressed and conclusions arrived at, are those of the authors and are not necessarily to be attributed to ABSA.

The financial assistance of the South African Department of Science and Technology (DST) towards this research is hereby acknowledged. Opinions expressed and conclusions arrived at are those of the authors, and are not necessarily to be attributed to DST.

Appendix

The different steps of the algorithm for a single radar scan are summarized in Figure 7.

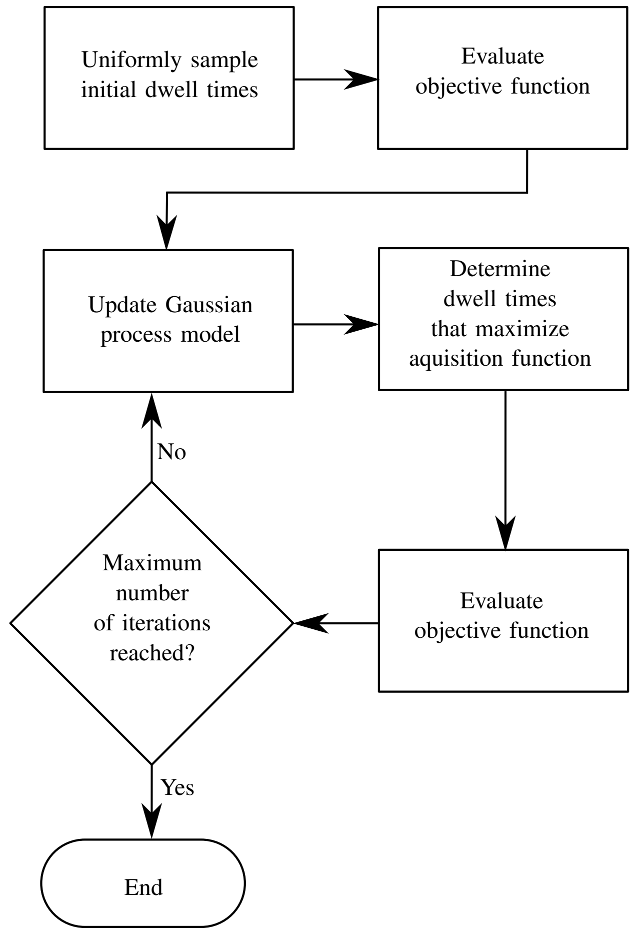

Fig. 7: Flow chart of the algorithm for a single radar scan.

References

[1] E. Blasch, J. Nagy, S. Scott, J. Okoth, and M. Hinman, "Physics-based and human-derived information fusion for analysts," *Proc. SPIE*, vol. 10207, pp. 10 207 – 10 207 – 12, 2017.

[2] P. Sgambato, N. Botta, S. Celentano, C. D. Dio, G. Marzano, O. Musio, and C. Petrillo, "System manager for AESA radar systems," in *2015 IEEE Radar Conference (RadarCon)*, May 2015, pp. 1734–1738.

[3] G. Galati, F. Madia, P. Carta, E. G. Piracci, S. Franco, and S. Quattrociocchi, "Time for a change in phased array radar architectures- part ii: The d-radar," in *2015 16th International Radar Symposium (IRS)*, June 2015, pp. 918–923.

[4] K. L. Bell, C. J. Baker, G. E. Smith, J. T. Johnson, and M. Rangaswamy, "Cognitive radar framework for target detection and tracking," *IEEE Journal of Selected Topics in Signal Processing*, vol. 9, no. 8, pp. 1427–1439, Dec 2015.

[5] S. F. Page, J. P. Oldfield, S. Islip, B. Benfold, R. Brandon, P. A. Thomas, and D. J. Stubbins, "Threat assessment and sensor management in a modular architecture," *Proc. SPIE*, vol. 9995, pp. 9995 – 9995 – 12, 2016.

[6] G. Box and K. Wilson, "On the experimental attainment of optimum conditions," *Journal of the Royal Statistical Society. Series B (Methodological)*, vol. 13, no. 1, pp. 1–45, 1951.

[7] D. R. Jones, "A Taxonomy of Global Optimization Methods Based on Response Surfaces," *Journal of Global Optimization*, vol. 21, no. 4, pp. 345–383, Dec 2001.

[8] J. Snoek, H. Larochelle, and R. Adams, "Practical Bayesian optimization of machine learning algorithms," in *Neural Information Processing Systems*, 2012.

[9] J. Sacks, W. J. Welch, T. J. Mitchell, and H. P. Wynn, "Design and analysis of computer experiments," *Statistical science*, pp. 409–423, 1989.

[10] G. Yildiz and S. Tunali, "Response surface methodology based simulation optimization of a conwip controlled dual resource constrained system," *The International Journal of Advanced Manufacturing Technology*, vol. 36, no. 11-12, pp. 1051–1060, 2008.

[11] H. Mansouri, M. Bannayan Aval, P. Rezvani Moghaddam, and A. Lakzian, "Management of nitrogen fertilizer, irrigation and plant density in onion production using response surface methodology as optimization approach," *African Journal of Agricultural Research*, vol. 9, 2014.

[12] R. Garnett, M. A. Osborne, and S. J. Roberts, "Bayesian optimization for sensor set selection," in *Proceedings of the 9th ACM/IEEE International Conference on Information Processing in Sensor Networks*, ser. IPSN '10. New York, NY, USA: ACM, 2010, pp. 209–219.

[13] R. Martinez-Cantin, N. de Freitas, E. Brochu, J. Castellanos, and A. Doucet, "A bayesian exploration-exploitation approach for optimal online sensing and planning with a visually guided mobile robot," *Autonomous Robots*, vol. 27, no. 2, pp. 93–103, 2009.

[14] Z. Ding, "A survey of radar resource management algorithms," in *Proc. Can. Conf. Electr. Comput. Eng.*, may 2008, pp. 001 559–001 564.

[15] N. Xiong and P. Svensson, "Multi-sensor management for information fusion: issues and approaches," *Inf. Fusion*, vol. 3, no. 2, pp. 163–186, 2002.

[16] S. Musick and R. Malhotra, "Chasing the elusive sensor manager," in *Proc. IEEE Natl. Aerosp. Electron. Conf.*, vol. 1, may 1994, pp. 606–613.

[17] G. Earl and B. Ward, "Frequency management support for remote sea-state sensing using the JINDALEE skywave radar," *IEEE J. Ocean. Eng.*, vol. 11, no. 2, pp. 164–173, apr 1986.

[18] Z. Wang, X. Wang, W. Moran, and Q. Pan, "An efficient sensor scheduling for multi-target localisation in MIMO radar networks," in *2015 16th International Radar Symposium (IRS)*, June 2015, pp. 1033–1038.

[19] G. Xiaojie and L. Wenchao, "Utilization of time resource for the dwell scheduling of the phase array radar," in *2016 CIE International Conference on Radar (RADAR)*, Oct 2016, pp. 1–5.

[20] P. Sgambato, S. Celentano, C. D. Dio, and C. Petrillo, "A flexible on-line scheduling algorithm for multifunctional radar," in *2016 IEEE Radar Conference (RadarConf)*, May 2016, pp. 1–5.

[21] M. Shaghaghi and R. S. Adve, "Task selection and scheduling in multifunction multichannel radars," in *2017 IEEE Radar Conference (RadarConf)*, May 2017, pp. 0969–0974.

[22] Q. Wang, T. Zhang, Y. Li, G. Cui, L. Kong, X. Yang, and J. Yang, "Tasks scheduling for multistatic radar network," in *2016 CIE International Conference on Radar (RADAR)*, Oct 2016, pp. 1–5.

[23] D. Khosla, D. J. Huber, and Y. Chen, "Automated scheduling of radar-cued camera system for optimizing visual inspection and detection of radar targets," in *2017 IEEE International Symposium on Technologies for Homeland Security (HST)*, April 2017, pp. 1–5.

[24] M. E. Gomes-Borges, D. Maltese, P. Vanheeghe, and E. Duflos, "A risk-based sensor management using random finite sets and pomdp," in *2017 20th International Conference on Information Fusion (Fusion)*, July 2017, pp. 1–9.

[25] Z. Liu, Y. Wang, and F. Zhong, "A scheduling method based on the adaptive order least square tracking filtering algorithm of phased array radars," in *2015 8th International Congress on Image and Signal Processing (CISP)*, Oct 2015, pp. 1152–1156.

[26] A. E. Mitchell, G. E. Smith, K. L. Bell, and M. Rangaswamy, "Single target tracking with distributed cognitive radar," in *2017 IEEE Radar Conference (RadarConf)*, May 2017, pp. 0285–0288.

[27] Z. Zhang and Y. Tian, "A novel resource scheduling method of netted radars based on markov decision process during target tracking in clutter," *EURASIP Journal on Advances in Signal Processing*, vol. 2016, no. 1, p. 16, Feb 2016.

[28] W. Sun, W. Yi, M. Xie, Y. Yuan, and L. Kong, "Adaptive node and power simultaneous scheduling strategy for target tracking in distributed multiple radar systems," in *2017 20th International Conference on Information Fusion (Fusion)*, July 2017, pp. 1–6.

[29] S. R. Martin and A. J. Newman, "The application of particle swarm optimization and maneuver automatons during non-Markovian motion planning for air vehicles performing ground target search," in *Proc. IEEE/RSJ Int. Conf. Intell. Robot. Syst.*, sept. 2008, pp. 2605–2610.

[30] P. J. Shea, J. Kirk, and D. Welchons, "Adaptive sensor management for multiple missions," in *Proc. SPIE Conf. Def. Secur.*, 2009, pp. 73 300M–73 300M–12.

[31] Z. Hao-wei, X. Jun-wei, and S. Chuan, "Scheduling method for phased array radar over chaos adaptively genetic algorithm," in *2016 Sixth International Conference on Information Science and Technology (ICIST)*, May 2016, pp. 111–116.

[32] L. Hao, X. Yang, and S. Hu, "Task scheduling of improved time shifting based on genetic algorithm for phased array radar," in *2016 IEEE 13th International Conference on Signal Processing (ICSP)*, Nov 2016, pp. 1655–1660.

[33] H.-w. Zhang, J.-w. Xie, W.-l. Lu, C. Sheng, and B.-f. Zong, "A scheduling method based on a hybrid genetic particle swarm algorithm for multifunction phased array radar," *Frontiers of Information Technology & Electronic Engineering*, vol. 18, no. 11, pp. 1806–1816, Nov 2017.

[34] S. Ahlberg, P. Hörling, K. Johansson, K. Jöred, H. Kjellström, C. Mårtenson, G. Neider, J. Schubert, P. Svenson, P. Svensson, and J. Walter, "An information fusion demonstrator for tactical intelligence processing in network-based defense," *Inf. Fusion*, vol. 8, no. 1, pp. 84–107, 2007, special Issue on the Seventh International Conference on Information Fusion – Part II.

[35] G. Grimmett and D. Stirzaker, *Probability and Random Processes*, 3rd ed. Oxford University Press, Oxford, UK, 2001.

[36] J. L. Williams, "Search theory approaches to radar resource allocation," in *Proc. 7th US/Australia Joint Workshop on Defense Applications of Signal Processing*, 2011.

[37] C. Rasmussen and C. Williams, *Gaussian processes for machine learning*. MIT Press Cambridge, 2006.

[38] G. Morris and L. Harkness, *Airborne Pulsed Doppler Radar*, 2nd ed. Artech House Inc., 1996.